GOCE SSTI L2 TRACKING LOSSES AND THEIR IMPACT ON POD PERFORMANCE

Jose van den IJssel[1], Pieter Visser[1], Eelco Doornbos[1], Ulrich Meyer[2], Heike Bock[2], and Adrian Jäggi[2]

[1]*Department of Earth Observation and Space Systems, Delft University of Technology, The Netherlands*
[2]*Astonomical Institute, University of Bern, Switzerland*

ABSTRACT

The state-of-the-art GOCE Satellite-to-Satellite Tracking Instrument (SSTI) delivers high-quality GPS data with an almost continuous 1 Hz data rate, which allows for very Precise Orbit Determination (POD). Despite this good performance, the GPS receiver shows occasional unexpected L2 tracking losses, which mainly occur close to the geomagnetic poles and, to a lesser extent, also along the geomagnetic equator. The number of unexpected L2 tracking losses varies in time and shows some correlation with solar activity. Less than 3% of the observation data is affected by these losses. Therefore, the effect on the POD remains limited. However, systematic effects might be present, as the quality of the GOCE orbits is slightly reduced over the polar regions. The striking correlation between the global distribution of ionospheric irregularities and L2 losses suggests scintillation effects might be present. Analysis of the time derivative of the geometry-free combination of GPS phase observations shows that unexpected L2 losses occur during times of rapid ionospheric fluctuations. GPS satellites in cross-track direction are most affected by L2 losses.

Key words: GOCE; GPS; tracking losses; ionosphere; scintillations.

1. INTRODUCTION

The Gravity field and steady-state Ocean Circulation Explorer GOCE[2] is the first Earth explorer core mission of the European Space Agency (ESA). It has been launched on March 17, 2009 from Plesetsk, Russia, into an exceptionally low Earth orbit with an initial altitude of about 280 km. The core instrument is a three-axis gradiometer for determining the gravity field with an unprecedented accuracy of 1 mgal and the geoid with an accuracy of 1 cm, both at a spatial resolution of 100 km [6]. In addition, the mission is equipped with two state-of-the-art Lagrange SSTIs, each consisting of a 12-channel dual-frequency GPS receiver connected to a helix antenna. The main unit (SSTA) is running in nominal operations, whereas the other one serves as redundant unit (SSTB). The GPS data are primarily used for the precise orbit determination of the satellite and the derivation of the long wavelength part of the Earth's gravity field.

The main SSTI delivers high-quality GPS data with an almost continuous 1 Hz data rate[1]. Despite this good performance, the GPS receiver shows occasional L2 tracking losses. Missing L2 observations at the begin and end of a GPS satellite pass are expected, due to receiver tracking technologies and a lower carrier-to-noise ratio. However, L2 losses occurring in the middle of a satellite pass are unexpected.

In this paper, the occurrence of the unexpected L2 tracking losses is investigated. An overview of the occurrence of L2 losses is given in section 2. In section 3 it is investigated whether these L2 losses might be due to ionospheric scintillation effects and in section 4 the possible impact of the L2 losses on the quality of the orbit determination is analyzed. Finally, section 5 summarizes the results.

2. OVERVIEW OF L2 LOSSES

Figure 1 shows that the amount of L2 losses varies in time. A satellite tracking pass starts with acquisition of the first L1 observation and continues, while the satellite is constantly in view of the receiver, until the last L1 observation. Figure 1 shows that L2 losses at the begin and end of such a pass affect around, respectively, 5 and 3% of the observations, indicating that it takes significantly longer for the second frequency to acquire lock compared to the first frequency. The second frequency also looses lock earlier than the first frequency. The number of unexpected L2 losses occurring in the middle of a pass in general is very low, with at most 3% of the observation data affected by these losses. Time series of the solar proxy $F_{10.7}$ and the geomagnetic index ap are also depicted, to investigate possible correlations between the L2 losses and the solar and geomagnetic activity. There seems to be some correlation between L2 losses and the solar activity, but this correlation is not very strong. There might also be a seasonal dependency, with more losses during winter times and less losses during summer. Unfortunately, a large amount of data during the summer months of 2010 is missing, which makes it difficult to clearly see the seasonal dependency.

Proc. of '4th International GOCE User Workshop', Munich, Germany
31 March – 1 April 2011 (ESA SP-696, July 2011)

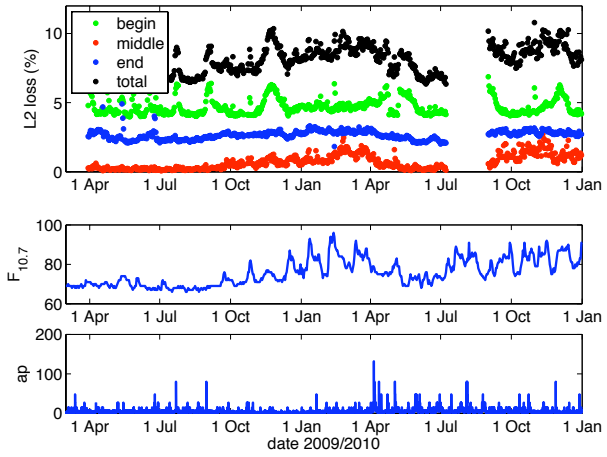

Figure 1. Overview of L2 losses occurring at the begin, middle and end of a pass as a function of time (top), together with time series of the solar activity proxy $F_{10.7}$ (center) and the geomagnetic index ap (bottom).

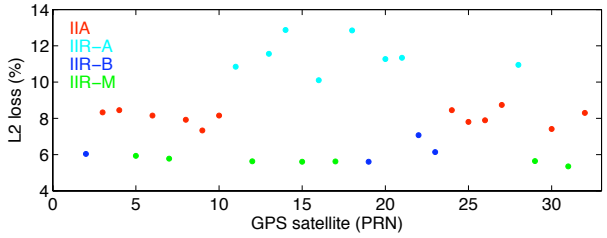

Figure 2. Overview of average L2 losses per GPS satellite using almost 20 months of GOCE data.

Figure 2 shows the relative amount of L2 losses for each individual GPS satellite that is tracked by GOCE. There is a clear correlation with the different block types of the GPS satellites. Block IIR-A satellites show the largest percentage of L2 losses, followed by block IIA satellites. Block IIR-B and IIR-M satellites are least affected by L2 losses. Because of the limited data available for block IIF satellites, data for this block type are not included in this figure. The L2 losses shown in figure 2 include the total amount of L2 losses occurring at the begin, middle and end of a pass. The large differences between the relative amount of L2 losses per GPS block type are predominantly due to L2 losses at the end of a pass. The occurrence of unexpected L2 losses during the middle of a pass is comparable for all GPS block types.

Figure 3 shows the geographical dependency of the unexpected L2 losses that occur in the middle of a pass. Most of these losses occur close to the geomagnetic poles. Dim bands with L2 losses are also visible along the geomagnetic equator. Because most losses occur near the poles, the losses are also shown in a polar projection. At the South pole, a ring structure is visible where the auroral oval is located. Due to the sun-synchronous orbit of the satellite, the distribution of GPS observations is relatively uniform in longitude, but varies with latitude. At

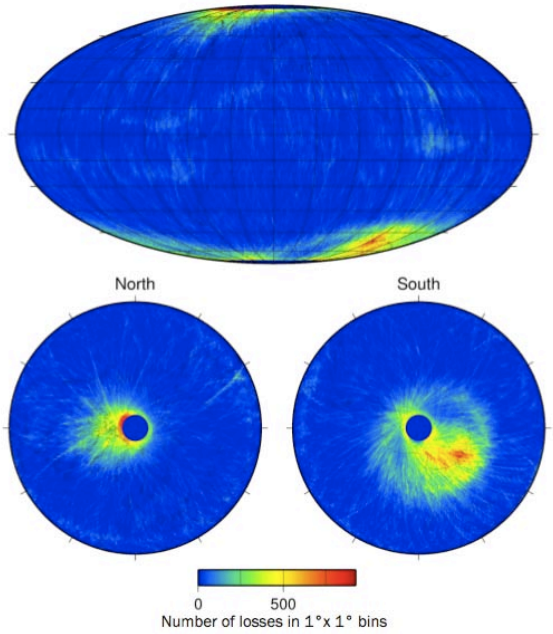

Figure 3. Distribution of unexpected L2 losses occurring in the middle of a pass in global view (top) and near the poles (bottom). Results are given in 1°x 1° bins using almost 20 months of GOCE data.

the poles, a small cap of around 7° is without data coverage. Due to the dense ground tracks near this polar gap, the number of GPS observation is highest close to the poles. However, this distribution of GPS observations can not fully explain the large number of L2 losses near the poles.

3. ANALYSES OF SCINTILLATION EFFECTS

The striking correlation between the global distribution of unexpected L2 losses shown in figure 3 and the occurrence of ionospheric irregularities shown in figure 4 suggests scintillation effects might be present. It is known that GPS receivers can suffer from ionospheric irregularities, which can cause rapid fluctuations in amplitude and phase of the signal. The rapid phase variations cause a doppler shift in the GPS signal which may exceed the bandwidth of the phase lock loop [5]. Additionally, amplitude fades can cause the signal-to-noise ratio (SNR) to drop below the receiver threshold, resulting in loss of code lock. These effects have a larger impact on tracking loops employing codeless and semi-codeless technologies to extract the encrypted L2 signal, compared to full code correlation. Due to the narrower bandwidth of the phase lock loop, the L2 frequency is more susceptible to phase scintillations [7].

To check the occurrence of amplitude fades the SNR on both frequencies are analyzed. The occurrence of phase scintillations is investigated by looking at the geometry-free combination of GPS observations. This combina-

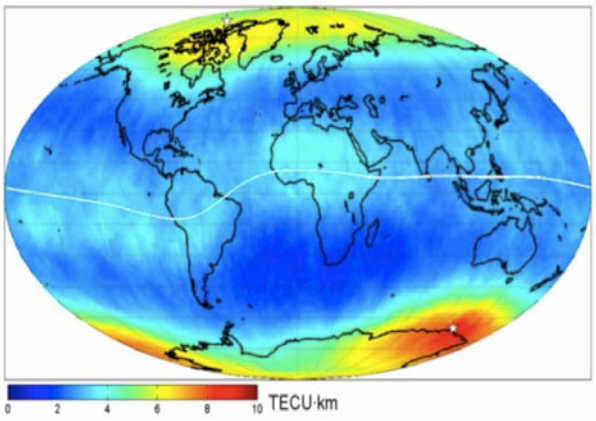

Figure 4. Global distribution of the occurrence of ionospheric irregularties (characteristic scale length about 15-30 km) detected by CHAMP data from March 2002 - February 2006 [4].

tion is independent of receiver and satellite clocks and geometry and gives an indication of the ionospheric effect. The geometry-free combination can be formed using the $P1$ and $P2$ pseudoranges, as well as the $L1$ and $L2$ phase observations. The GPS frequencies are f_1 = 1575.42 MHz and f_2 = 1227.60 MHz. Equations 1 to 5 give an overview of all geometry-free combinations that have been investigated in this study. The geometry-free combination of code observations P_{GF} gives an indication of the ionospheric delay. Unfortunately, this combination also contains possible multipath effects, as well as receiver and satellite dependent differential biases, due to the fact that the two GPS frequencies undergo different propagation delays inside the receiver and satellite hardware. Furthermore, this combination suffers from the relatively large noise level of the code observations. The geometry-free combination of the phase observations L_{GF} also includes the ionospheric delay and is significantly less noisy. However, carrier phase ambiguities are present in this combination. The time derivative of the geometry-free combination of phase observations ΔL_{GF} allows to monitor the time variation of the ionospheric delay. This combination does not contain the ambiguity, as long as no cycle slips occur. Unfortunately, observations on both frequencies are required to compute these combinations. During times of L2 losses, it is not possible to compute these combinations and therefore also the geometry-free combination of code and phase measurements C_{GF} has been investigated. This combination uses only data on the L1 frequency and gives an indication of the ionospheric delay, as well as the other effects mentioned above. The noise level of this combination is roughly half the code noise. The time derivative of this combination ΔC_{GF} gives information about the ionospheric variations.

$$P_{GF} = P1 - P2 \quad (1)$$

$$L_{GF} = L1 - L2 \quad (2)$$

$$\Delta L_{GF} = \frac{L_{GF}(t_2) - L_{GF}(t_1)}{t_2 - t_1} \quad (3)$$

$$C_{GF} = (P1 - L1)/2 \quad (4)$$

$$\Delta C_{GF} = \frac{C_{GF}(t_2) - C_{GF}(t_1)}{t_2 - t_1} \quad (5)$$

Figure 5 shows results for a selection of these combinations of GPS observations for a short time period on 17 January 2011, when data from both the main (SSTA) and the redundant (SSTB) GPS receiver are available. Data from both receivers are analyzed, to investigate whether the occurrence of L2 losses is receiver dependent. During the selected time period, the GOCE satellite tracks 10 GPS satellites. All results shown in figure 5 are based on tracking observations from GPS satellite G30. The bottom figure shows the latitude of the GOCE satellite in black, with L2 losses at the begin, middle and end of a pass indicated in, respectively, green, red and blue. The unexpected L2 losses in red occur at high latitude, when the satellite is close to the pole. The elevation of the tracked G30 satellite is shown in gray. For this particular GPS satellite the elevation remains quite low, with a maximum elevation angle of 23°. The top figure shows for both receivers the SNR on two frequencies. Results for both receivers are very similar. Around the time of the unexpected L2 losses there is a small drop in SNR at the first frequency (S1), however, the SNR on the second frequency (S2) shows no degradation around these losses. The next figure shows the geometry-free combination of phase observations L_{GF}. As expected, many cycle slips are visible around the time of the L2 losses, which make it difficult to determine the ionospheric delay. This figure also shows that the redundant receiver looses lock at the end of the pass earlier than the main receiver. This behavior can be seen for all periods when tracking data for both receivers are available. At the beginning of each pass, the redundant receiver also needs more time to acquire lock than the main receiver, resulting in significantly more tracking data obtained with the main receiver compared to the redundant receiver. However, the amount of L2 losses in the middle of a pass is more or less comparable for both receivers. The next figure shows the time derivative of the geometry-free combination of phase observations ΔL_{GF}. Due to the 1 Hz data rate of the GOCE GPS observations, it is possible to see very rapid ionospheric variations. A remarkable increase in ionospheric fluctuations is visible around the time of L2 losses. It is stressed that at the actual times of L2 losses, the ΔL_{GF} can not be determined. When the satellite flies over the geomagnetic equator, ionospheric variations are also visible. Although these variations can be rather large, they are in general quite smooth. It seems that such smooth variations are less likely to result in L2 losses than the more rapid fluctuations at the poles. The next figure shows the time derivative of the geometry-free combination of code and phase observations, which can also be computed at times of L2 losses. Because the P1 code is also unavailable at times of L2 losses, the C/A code observation is used in this combination. Unfortunately, the C/A code is too noisy to see the ionospheric variations with this combination.

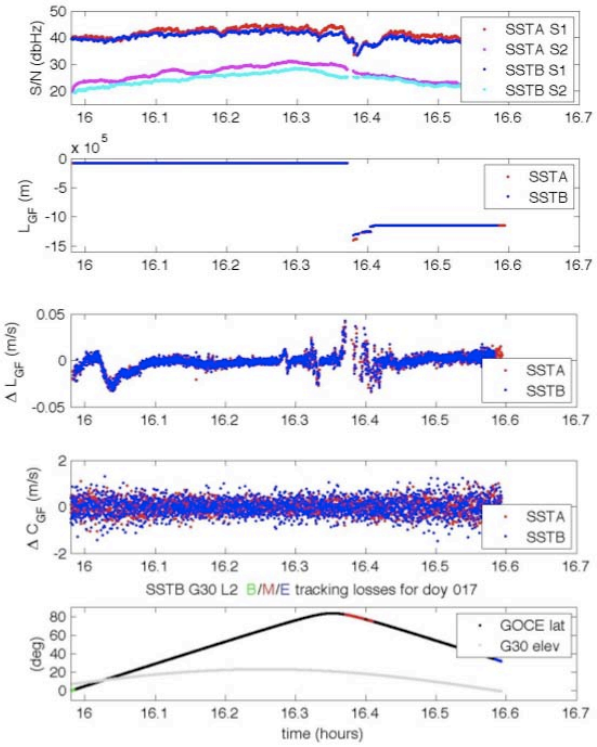

Figure 5. Analysis of several GOCE GPS tracking observables for G30 on 17 January 2011 using the main (SSTA) and redundant (SSTB) receiver.

The analysis carried out for satellite G30, shown in figure 5 has been repeated for all GPS satellites that are tracked by the GOCE satellite during the selected period. The left part of figure 6 shows for all 10 GPS satellites the time derivative of the geometry-free combination of GPS phase observations ΔL_{GF} during a short 12-minute time period when GOCE flies over the North pole. For a clear picture, the results for each GPS satellite are incremented by 0.1 m/s and the satellites are ordered depending on the level of ionospheric disturbances, with lowest variations for the top satellite and largest variation for the lower satellites. The right part of figure 6 shows for each GPS satellite the corresponding latitude of the orbit. Again, for clarity, the results per GPS satellite are incremented by 40°. L2 losses occurring at the begin, middle and end of a pass are again indicated on the latitude of the orbit in respectively green, red and blue. There is a clear correlation between the level of ionospheric disturbances and the presence of unexpected L2 losses. All results shown in figure 6 are obtained with the redundant GPS receiver. Analysis of the main GPS receiver shows comparable results, which are not included in this figure.

Figure 7 shows for the same 12-minute time period analyzed in the previous figure the respective ground tracks of GOCE and the 10 tracked GPS satellites. GPS satellites that are tracked without L2 losses are indicated in dark blue, while GPS satellites shown in light blue indicate that unexpected L2 tracking losses occur. From this figure, it seems that GPS satellites in cross-track direction

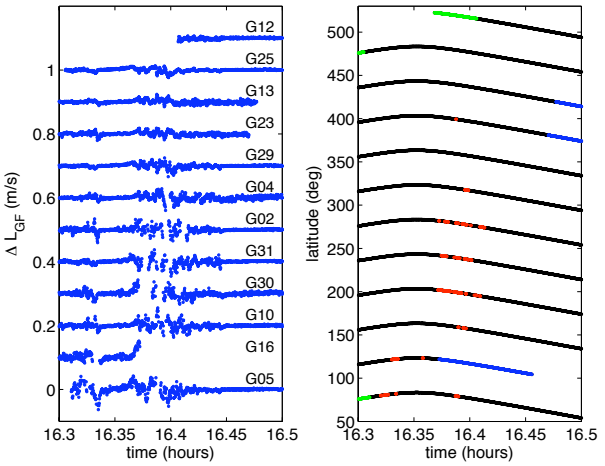

Figure 6. Overview of ΔL_{GF} for 10 GPS satellites tracked by the redundant GPS receiver for a 12-minute period on 17 January 2011 (left) and their corresponding latitudes (right) with L2 losses at the begin, middle and end of a pass indicated in respectively green, red and blue. For clarity the ΔL_{GF} and latitude results for each GPS are incremented by respectively 0.1 m/s and 40°.

are more prone to L2 losses than GPS satellites in along-track direction. This might indicate that the ionospheric disturbances during this 12-minute period are located to both sides of the GOCE ground track, or maybe the helix antenna is more sensitive to this effect for GPS satellites located sideways of GOCE.

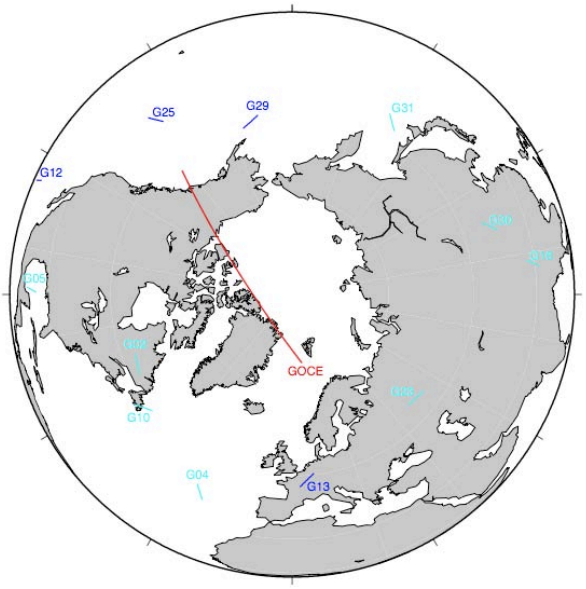

Figure 7. Ground tracks of GOCE and 10 tracked GPS satellites for a 12-minute period on 17 January 2011 when GOCE flies over the North pole.

To see whether the tracking of GPS satellites located sideways to GOCE is systematically more affected by L2 losses, figure 8 shows an azimuth-elevation diagram of

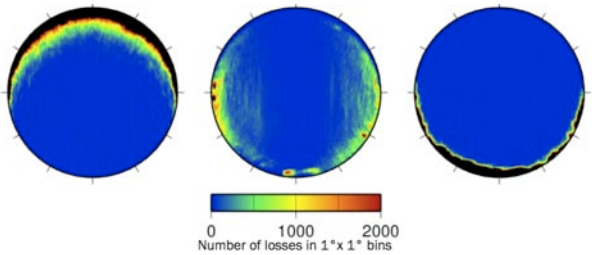

Figure 8. Azimuth-elevation diagram of L2 losses occurring at the begin (left), middle (center) and end (right) of a pass in 1°x 1° bins in the antenna-fixed frame using 1 year of GOCE data. The flight direction is upwards.

the L2 losses in the antenna-fixed frame based on one year of GOCE data. The azimuth is counted clockwise, with the flight direction pointing upwards. The elevation is 0° at the outer border and 90° in the center of the plot. L2 losses at negative elevation angles are not taken into account in this figure. For clarity, the scaling of the L2 losses at the begin and end of a pass is adjusted to the number of L2 losses occurring in the middle of a pass. Figure 8 shows that the occurrence of unexpected L2 losses in the middle of a pass is dependent on azimuth and elevation. Most losses occur at lower elevations and hardly any losses are present at the highest elevations. This can be explained by the fact that the unexpected L2 losses predominantly occur at the poles and in this region there are no observations at elevations larger than 55°, due to the orbit geometry of the GPS constellation. As expected, L2 losses occurring at the begin and end of a pass can be found at low elevations in, respectively, the flight and aft direction of the satellite. Therefore, there are hardly any unexpected L2 losses at low elevations around azimuth angles of 0 and 180°. However, this does not fully explain why at medium elevations there are significantly more unexpected L2 losses for GPS satellites located sideways of GOCE, which means that specific antenna characteristics like e.g. multipath might also play a role.

4. IMPACT ON POD PERFORMANCE

Figure 1 shows that less than 3% of the GPS observations is affected by unexpected L2 losses occurring in the middle of a pass. With such a relatively small amount, the impact on the POD remains limited. Bock et al. [1] have shown that state-of-the-art precise science orbits are computed for the GOCE satellite, with an orbit accuracy at the 2 cm level, validated by independent Satellite Laser Ranging (SLR) measurements. However, figure 9 shows that the quality of these GOCE orbits is slightly reduced over the polar regions, which also affects GPS-based gravity field recovery as shown by [3]. RMS differences of up to 5 cm are visible between the reduced-dynamic and kinematic PSO over the geomagnetic poles, which can be attributed to a reduced quality of the kinematic orbits, as they are more affected by the

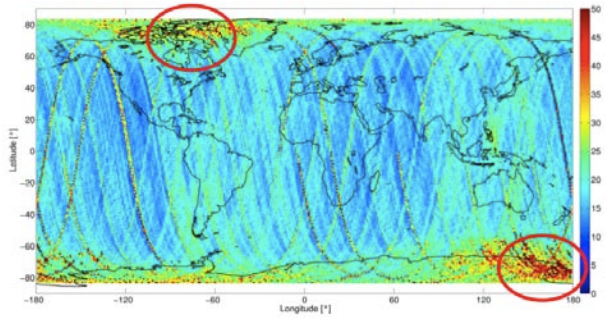

Figure 9. Global distribution of the RMS of the differences between the reduced-dynamic and kinematic Precise Science Orbits (PSO) in (mm).

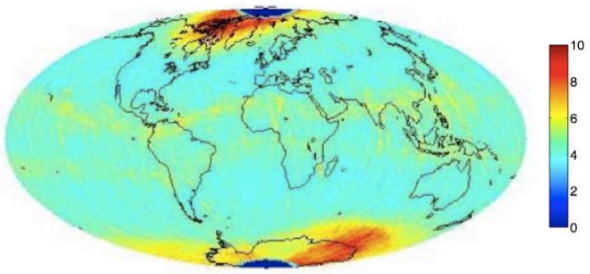

Figure 10. Global distribution of the RMS of the reduced-dynamic PSO phase residuals in (mm) for 2010.

quality of the observation data. Furthermore, figure 10 shows that the ionospheric-free combination of phase observations used for the reduced-dynamic PSO computations show systematically larger residuals close to the geomagnetic poles and, to a lesser extent, also along the geomagnetic equator. It is known that the observation geometry of the GPS constellation is slightly worse near the poles. However, due to the fact that the reduced orbit quality is visible near the geomagnetic poles, instead of the poles in general, it is clear that the reduced GPS observation geometry at the poles can not fully explain this effect. The strong correlation with the global distribution of the unexpected L2 losses occurring in the middle of a pass seems to suggest that these losses contribute to the reduced quality of the GOCE orbits at the polar regions. However, other effects that are correlated with increased ionospheric variations, e.g. higher order ionospheric terms that are so far ignored in the POD, might also play a role.

5. CONCLUSIONS

The GOCE SSTI delivers high-quality GPS data with an almost continuous 1 Hz data rate, but suffers from occasional unexpected L2 losses in the middle of a tracking pass. An overview of the occurrence of these L2 losses is presented, which shows that the relative amount of tracking losses varies in time and that these variations show some correlations with the solar activity. Most unex-

pected L2 losses occur close to the geomagnetic poles and, to a lesser extent, also along the geomagnetic poles. Analysis using several geometry-free combinations of GPS observations from the main as well as the redundant SSTI points to an influence of the ionosphere on the signal reception of the GPS antenna. A clear correlation is visible between the level of ionospheric disturbances and the presence of unexpected L2 losses. It is shown that the tracking of GPS satellites located sideways to GOCE is systematically more affected by L2 losses. With less than 3% of the GPS data affected by these unexpected L2 losses, the impact on the POD remains limited. However, the quality of the GOCE orbits is slightly reduced over the areas where most L2 losses occur, suggesting that systematic effects might be present.

ACKNOWLEDGMENTS

The authors acknowledge the European Space Agency (ESA) for the provision of the GOCE data. Significant parts of this work are financed through ESA contract no. 18308/04/NL/MM for the design, development and operation of the GOCE Level 2 data processing system.

REFERENCES

[1] Bock H., Jäggi A., Meyer U., Visser P., Van den IJssel J., Van Helleputte, T., Heinze M., Hugentobler U., 2011, GPS-derived orbits for the GOCE satellite, submitted to J. Geod

[2] Drinkwater M., Muzzi D., Popescu A., Floberhagen R., Kern M., Fehringer M., 2006, The GOCE gravity mission: ESA's first core explorer, In: Proceedings of the 3rd GOCE User Workshop, 6-8 November 2006, Frascati, Italy, ESA SP-627, 1–7

[3] Jäggi A., Bock H., Meyer U., GPS-only gravity field recovery from GOCE, In: Proceedings of the 4th GOCE User Workshop, 31 March - 1 April, Munich, Germany

[4] Jakowski N., Mayer C., Wilken V., 2006, GPS Sounding of the Ionosphere Onboard CHAMP, In: Characterising the ionosphere, Meeting proceedings RTO-MP-IST-056, Paper 26, France

[5] Leick A., 1995, GPS Satellite Surveying, second edition, John Wiley and Sons, USA

[6] Rummel R., Balmino G., Johannesen J., Visser P., Woodworth P., 2002, Dedicated gravity field missions–principles and aims, J Geodyn 33, 3–20

[7] Skone S., Knudsen K., de Jong M., 2001, Limitations in GPS Receiver Tracking Performance Under Ionospheric Scintillation Conditions, Phys Chem Earth (A) 26(6-8), 613–621